Journal of Hepatocellular Carcinoma

Dovepress
Taylor & Francis Group

Open Access Full Text Article

ORIGINAL RESEARCH

AI-Based Quantification of Enhancing Tumor Volume on Contrast-Enhanced MRI to Predict Pathologic Response and Prognosis in HCC After HAIC Plus Targeted Therapy and Immunotherapy

Yin Zhou[1,*], Junjie Li[2,*], Qingshu Li[3,*], Liu Liu[1], Ping Huang[4], Yun Mao[1], Yaying Yang[3], Furong Lv[1], Ziyu Liu[1]

[1]Department of Radiology, The First Affiliated Hospital of Chongqing Medical University, Chongqing, 400016, People's Republic of China; [2]Department of Nuclear Medicine, The First Affiliated Hospital of Chongqing Medical University, Chongqing, People's Republic of China; [3]Department of Pathology, School of Basic Medicine, Chongqing Medical University, Molecular Medicine Diagnostic and Testing Center, Chongqing Medical University, Department of Clinical Pathology Laboratory of Pathology Diagnostic Center, Chongqing Medical University, Chongqing, 400016, People's Republic of China; [4]Department of Hepatobiliary Surgery, The First Affiliated Hospital of Chongqing Medical University, Chongqing, People's Republic of China

*These authors contributed equally to this work

Correspondence: Ziyu Liu, Master of Medicine, Department of radiology, the first affiliated hospital of Chongqing medical university, No. 1, Youyi Road, Yuzhong District, Chongqing, People's Republic of China, 400016, Tel +19942338328, Email liuziyu301@163.com

Purpose: To explore the diagnostic and prognostic value of AI-quantified MRI tumor volume for assessing pathologic response in unresectable hepatocellular carcinoma (uHCC) after hepatic arterial infusion chemotherapy plus targeted therapy and immunotherapy (HAIC-TI).

Materials and Methods: This retrospective study included 35 patients (46 lesions) who underwent HAIC-TI followed by hepatectomy. AI was used to calculate the tumor enhancement volume ratio (TEVR) from MRI. Correlation analysis was conducted to evaluate the relationship between TEVR and pathological tissue proportions. Receiver operating characteristic (ROC) curve determined the optimal cutoff for the ratio of viable tumor cells (RVTCs) to define major pathological response (MPR). The diagnostic performance of AI for MPR and its prognostic significance in recurrence-free survival (RFS) were assessed.

Results: TEVR in portal venous phase is strongly correlated with non-necrotic tissue ratio ($r = 0.89$, $p < 0.001$). RVTCs $\leq 10\%$ predicted reduced intrahepatic recurrence (Area Under the Curve [AUC] = 0.808, $p < 0.001$) and independently associated with prolonged RFS (HR [hazard ratio] = 0.19, 95% CI [confidence interval]: 0.05–0.69, $p = 0.011$). TEVR $\leq 19.5\%$ in the portal venous phase demonstrated high diagnostic performance for identifying MPR (AUC = 0.879) and was significantly associated with improved RFS in both univariable analysis (HR = 0.34, 95% CI: 0.12–1.00, $p = 0.049$) and the multivariable model incorporating only clinical and imaging factors.

Conclusion: AI-based MRI quantification of TEVR effectively reflected pathologic response and served as a non-invasive prognostic marker for postoperative recurrence in uHCC patients after HAIC-TI.

Plain Language Summary: Why was this study done? After receiving combined chemotherapy, targeted therapy, and immunotherapy for liver cancer, doctors need to accurately assess whether the tumor is responding well. Currently, this requires surgically removing the tumor for microscopic examination (pathological analysis), which cannot provide real-time evaluation during treatment. We aimed to use artificial intelligence (AI) to predict treatment effectiveness earlier using routine MRI scans, helping clinicians decide optimal timing for surgery.

What did we do? We analyzed data from 35 liver cancer patients treated with this combination therapy. An AI tool measured the tumor enhancement volume ratio (TEVR) on MRI scans and compared it with post-surgery pathology results. We focused on two questions: 1) Can TEVR reflect the proportion of surviving tumor cells? 2) Can TEVR predict postoperative recurrence risk?

Received: 25 March 2025
Accepted: 16 July 2025
Published: 21 July 2025

What did we find? AI-measured TEVR strongly matched pathology findings: When TEVR ≤ 19.5%, tumors had ≤10% surviving cells (indicating major treatment response), with 87.9% accuracy in predicting liver recurrence. Patients meeting this threshold had 5 times longer recurrence-free survival time (81% lower risk). This AI method works faster than traditional approaches and avoids additional procedures.

Keywords: hepatocellular carcinoma, hepatic arterial infusion chemotherapy, HAIC, targeted therapy and immunotherapy, MRI, pathologic response, artificial intelligence, AI

Key Point

1. MPR defined as RVTCs ≤ 10% can predict longer RFS.
2. Portal venous phase TEVR (≤19.5%) can predict MPR.
3. Portal venous phase TEVR (≤19.5%) can independently predicted longer RFS, preoperatively.

Introduction

Hepatocellular carcinoma (HCC) is among the second to fourth leading causes of cancer-related mortality worldwide.[1,2] More than 70% of HCC patients are diagnosed at an unresectable stage.[3] Conversion therapy, which integrates locoregional and systemic treatments, has emerged as a strategy to downstage tumors, allowing select patients to undergo resection and potentially improving survival outcomes.[3,4] Targeted therapies (TKIs) and immune checkpoint inhibitors (ICIs) have improved objective response rates (ORRs) and conversion surgery rates in unresectable HCC (uHCC).[4–8]

Hepatic arterial infusion chemotherapy (HAIC) is a locoregional treatment that delivers high-dose chemotherapy directly to liver tumors, achieving tumor control with manageable adverse effects.[9–11] HAIC is particularly beneficial for patients with portal vein invasion, liver dysfunction unsuitable for systemic therapy, or progressive disease following systemic treatment.[9–18] HAIC plus targeted therapy and immunotherapy (HAIC-TI) has demonstrated a superior ORR and an increased conversion rate in uHCC.[4,14,19,20] But when to perform surgery after conversion therapy remains a challenge for clinicians.

Pathological complete response (pCR) has been demonstrated as a stronger predictor of overall survival (OS) and recurrence-free survival (RFS) in patients undergoing locoregional therapy.[21,22] A study on transarterial chemoembolization (TACE) indicates that achieving pCR is significantly associated with improved OS ($p < 0.001$). Moreover, patients with ≥90% pathological response demonstrate superior OS and RFS compared to those with partial or no response ($p < 0.05$).[22] Similarly, in patients receiving TKIs and ICIs therapy for uHCC, those achieving pCR show significantly lower recurrence rates (6.7%) compared to non-pCR patients (40%) within a 13.2-month follow-up period.[23]

Given the strong correlation between pathological response and survival outcomes, therefore, accurate preoperative prediction of pathological response is crucial for optimizing treatment strategies in uHCC, which can affect the timing of surgery. However, due to the low conversion surgery rate in uHCC, postoperative pathological assessment remains limited, and pathology-imaging and prognostic correlation studies were restricted. Modified response evaluation criteria in solid tumors (mRECIST) based on CT or MRI images was most commonly applied for tumor response of uHCC conversion therapies, because it can assess the enhancing viable tumor area rather than only measurement of changes in tumor size obtained by RECIST version 1.1.[10,14,15,18,24,25] The accuracy of mRECIST in predicting pathological response is 63.6%, with a sensitivity of 76.2% and a specificity of 71.1%, in HCC after TACE.[26] Among patients achieving radiologic complete response (CR), 49% still have residual viable tumors on pathology.[21] While, the relationship between imaging-based response and pathological response after HAIC-TI, as well as their association with prognosis, remains to be further explored. Furthermore, the impact of HAIC-TI on overall tumor size and enhancement characteristics remains unclear. Since tumor response patterns often exhibit non-spherical and asymmetrical changes, one-dimensional measurement methods, such as mRECIST criteria, may be insufficient to fully capture the tumor's biological behavior.[27] Additionally, post-treatment, the enhanced portions of the lesion may become irregular in shape or exhibit atypical enhancement patterns, leading to poor measurement reproducibility.[25]

Due to the limitations of conventional response assessment criteria, volumetric quantification of enhancing tumor burden has emerged as a promising strategy to improve the reproducibility and prognostic accuracy of imaging biomarkers in locoregional therapies for HCC. A previous study has demonstrated that semiautomated three-dimensional (3D) analysis of contrast-enhanced MRI and quantitative apparent diffusion coefficient (qADC) maps exhibited strong correlation with histopathologic tumor necrosis following TACE,[27] thereby laying the groundwork for volumetric response assessment. In addition, enhancement-based imaging biomarkers such as enhancing tumor volume and enhancing tumor burden, derived via semiautomated segmentation, have shown utility in refining prognostic stratification within the Barcelona Clinic Liver Cancer (BCLC) staging system and guiding treatment decisions in intermediate- and advanced-stage HCC.[28] Building upon these foundations, recent advances in deep learning (DL) have enabled fully automated, high-throughput tumor segmentation,[29,30] offering potential improvements in accuracy, standardization, and clinical applicability for imaging-based assessment of tumor burden. A DL-based 3D convolutional neural network (3D U-Net) model has been validated for automated segmentation of Couinaud liver segments on portal venous phase MRI, achieving a mean dice similarity coefficient (DSC) of 90.2% and demonstrating high efficiency and cross-vendor robustness. Additionally, the automated segmentation process required only 8 seconds per case, compared to approximately 26 minutes for manual annotation, supporting its feasibility for clinical implementation.[29] Based on this algorithm, an AI-driven volumetric analysis tool has been applied to assess total tumor burden and predict early postoperative recurrence in HCC patients, showing high prognostic performance in resectable BCLC stage A and B cohorts.[31] However, these approaches have largely focused on treatment stratification in intermediate- and advanced-stage HCC—primarily to identify candidates for TACE—or on predicting early postoperative recurrence in patients with resectable HCC (BCLC stage A or B). In contrast, the potential relationship between contrast-enhancing tumor volume and pathological response or survival outcomes has not been systematically investigated in patients with uHCC undergoing multimodal conversion therapies such as HAIC-TI. Integrating AI-based volumetric tools into the clinical workflow for HAIC-TI may improve the accuracy of treatment response assessment and facilitate more informed decision-making in patients with uHCC.

Therefore, this study aimed to evaluate AI-based quantitative analysis of enhancing tumor volume from contrast-enhanced MRI for predicting pathological response and prognosis in patients with uHCC undergoing HAIC-TI.

Materials and Methods

Patients

Patients with initial uHCC who underwent HAIC-TI followed by hepatectomy in the First Affiliated Hospital of Chongqing Medical University between September 2020 and September 2024 were retrospectively analyzed. During the treatment process, all patients were discussed by the multidisciplinary team. Inclusion criteria: (1) Patients diagnosed with HCC through imaging or pathology, including those with major vascular invasion but without distant metastasis at initial diagnosis; (2) Patients who received at least one cycle of HAIC-TI as conversion therapy were successfully converted to meet hepatectomy criteria and subsequently underwent curative surgical resection with available pathological evaluation; (3) Patients who underwent contrast-enhanced MRI within two weeks before surgery. Exclusion criteria: (1) Incomplete preoperative contrast-enhanced MRI, defined as missing arterial, portal venous, or delayed phases, or images with severe motion or artifacts compromising diagnostic quality; (2) Inaccurate tumor segmentation, defined by any of the following conditions: (a) tumor region of interest (ROI) included non-tumoral liver tissue; (b) tumor ROI failed to encompass the entire tumor volume; (c) tumor ROI contained more than one HCC lesion.

HAIC-TI Protocol

The standard HAIC regimen utilized the FOLFOX protocol, combined with several protocols of targeted therapy and immunotherapy. Supplemental materials (E1) provide the concrete proposal.

Assessment of Response to HAIC and Follow-Up

After every 2–3 circles HAIC treatment, contrast-enhanced CT or MRI examination, along with chest CT, were performed to evaluate the efficacy of HAIC using mRECIST criteria.[24,25] Based on the result of mRECIST, patients

were divided into response group (CR + PR) and non-response group (SD + PD). Additionally, laboratory tests for tumor markers and liver function were conducted during the follow-up. Follow-up was conducted through telephone interviews, outpatient visits, and hospitalization records, every three months, continuing until January 30, 2025. Follow-up ended upon local recurrence, distant metastasis, or death, with the termination time recorded. RFS (including intrahepatic recurrence and metastasis to other organs) was calculated from the surgery date to recurrence, death, or last follow-up, with cases without events at the last visit considered censored.

MRI Acquisitions

MRI was performed with 3.0T system (Signa HD Excite; GE Healthcare, Milwaukee, WI) by using a phased array torso coil with 8 channels. MR imaging at least contained a axial pre- and post-contrast fat-suppressed three-dimensional (3D) T1-weighted liver acquisition with volume acceleration-extended volume (LAVA-XV) sequence [TR/TE, 4/1.9 ms; flip angle, 12°; slice thickness, 4 mm; intersection gap, 0 mm; acquisition matrix, 320 × 256; field of view, 400 × 340 mm]. Post-contrast images were acquired at different time points after contrast agents injected: early arterial phase (20–25 s), late arterial phase (40–45 s), portal venous phase (65–70 s), transitional phase (3–5 min), and hepatobiliary phase (HBP) (10–20 min). The hepatobiliary MRI contrast agents (Gadoxetic Acid Disodium Injection; Chiatai Tianqing Pharma, Jiangsu, China) was injected at a dosage of 25 μmol/kg body weight at a rate of 1 mL/s, followed by a 20-mL saline flush.

Preparation Prior to AI-Based Automated Segmentation

Before initiating automated segmentation, one radiologist (Z.Y.L.) reviewed all MR images on the AI software platform to confirm the accuracy of sequence labeling, HCC lesion localization, and the corresponding 3D bounding boxes generated by the system's automated lesion detection module, without any manual corrections. This step ensured that subsequent segmentation and volumetric quantification were based on anatomically valid inputs.

AI-Based Automated MRI Tumor and Enhancement Volume Analysis

The MRI automated image segmentation and volumetric quantification analyses were performed using commercial software (LiverMRDoc; version 2.10.0; SHU KUN) (Figure 1). Automated segmentation of HCC lesions and liver parenchyma was conducted on each MRI sequence using deep learning algorithms based on a 3D U-Net architecture.[29,31] The volume segmentation mask obtained from the optimal sequence determined automatically by the AI software was used to quantify the tumor volume (cm^3), with enhancement volumes calculated for both the arterial and portal venous phases, and the tumor enhancement volume ratio (TEVR) subsequently computed. TEVR = tumor enhancement volume/tumor volume × 100. For pathological correlation analysis, each lesion was analyzed individually to establish a one-to-one correspondence between TEVR and the proportion of pathological components. In contrast, for prognosis analysis, the overall tumor burden was used, with the sum of the enhancement volumes and tumor volumes of all lesions employed to calculate the overall TEVR.

Quality Control for AI-Based Tumor Segmentation

Two radiologists (Y.Z., with 10 years of experience in abdominal imaging, and Z.Y.L., with 7 years of experience) independently and visually assessed the accuracy of the automated tumor segmentation masks. Any discrepancies were resolved by consensus through discussion. Segmentations that met any of the exclusion criteria defined in Section 2.1 were excluded from the volumetric analysis. Notably, the subsequent segmentation masks were generated fully automatically and were not manually modified, as the objective of this study was to evaluate the prognostic utility of a fully automated, end-to-end AI workflow for tumor segmentation and volumetric analysis.

Pathologic Evaluation

All lesions visible on the final preoperative contrast-enhanced MRI, including both enhancing and necrotic regions, were reviewed by a multidisciplinary team (MDT). Radiologists numbered the lesions by location and size, and annotated the enhancing and necrotic regions, which were subsequently marked by surgeons during hepatectomy to guide pathological sampling. Gross specimens were evaluated to ensure spatial consistency between imaging findings and pathological sampling sites. A pathologist with 15 years of experience, blinded to clinical and imaging data, independently reviewed all resected

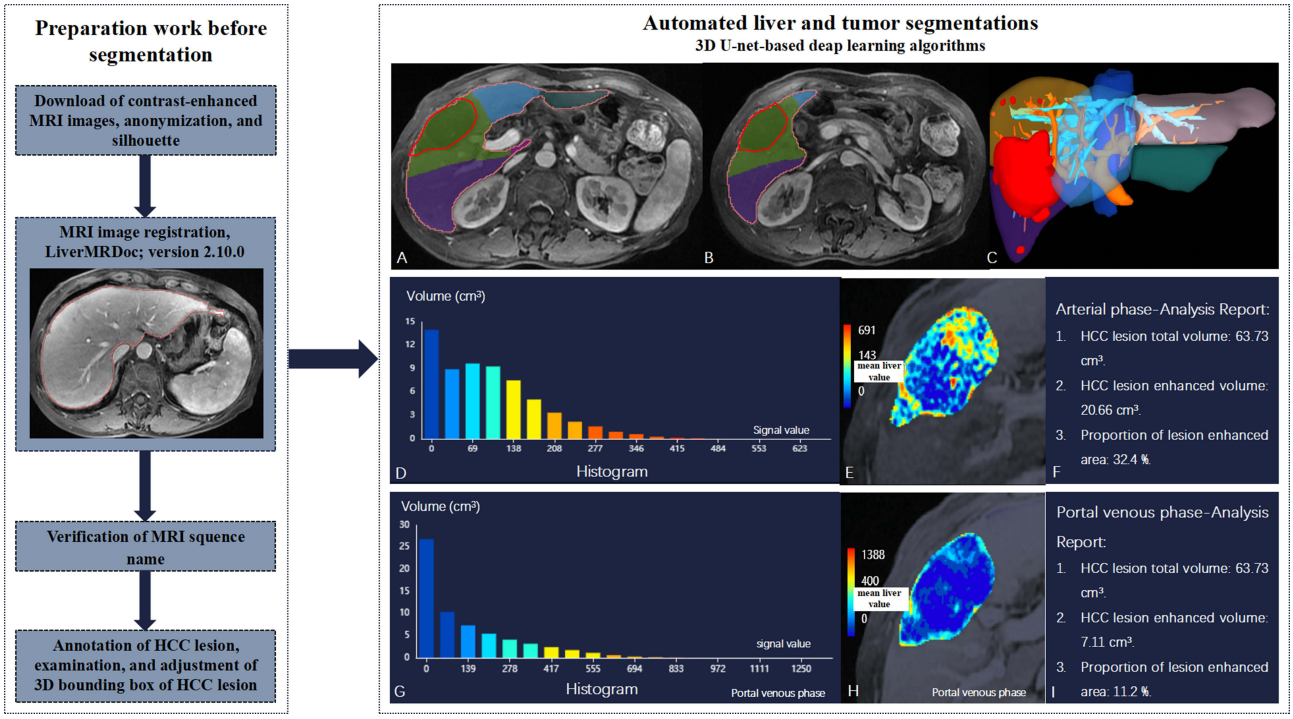

Figure 1 Workflow of automated segmentation and volumetric quantification analyses. (**A**–**I**) A representative case of automated segmentation. Axial T1-weighted portal venous phase images of a 52-year-old man showed a 65 mm HCC (*) in segment V. (**A**–**C**) Automated segmentations of the tumor (red lines) and liver (other colored lines) to create corresponding segmentation masks. (**D**–**E**) Histogram and pseudo-color map of the tumor's enhancement volume in the arterial phase. (**F**) Arterial phase analysis report showing total tumor volume (63.73 cm³), enhancement volume (20.66 cm³), and enhancement volume ratio (32.4%). (**D**–**H**) Histogram and pseudo-color map of the tumor's enhancement volume in the portal venous phase. (**I**) Portal venous phase analysis report showing total tumor volume (63.73 cm³), enhancement volume (7.11 cm³), and enhancement volume ratio (11.2%). HCC, hepatocellular carcinoma.
Abbreviations: MRI, magnetic resonance imaging; 3D U-net-based, three-dimensional convolutional neural network-based.

specimens. Pathological response was assessed by calculating the residual viable tumor (RVT) percentage, defined as the area of viable tumor under 100× magnification divided by the total area of the tumor bed. If no viable tumor cells were identified in the initially sampled sections, additional sections were obtained for confirmation. The number of additional samples was determined based on tumor bed size and pathology department capacity. Based on the presence or absence of viable tumor cells, each lesion was classified as either pCR (no viable tumor cells) or pathological partial response (pPR). The tumor bed in resected HCC specimens was evaluated for three components: residual viable tumor, necrotic areas, and tumor stroma (including fibrous tissue and inflammatory cells), with the sum of these components totaling 100%.[9,32] The proportion of each component was estimated in 5% increments through visual assessment. For each lesion, the mean proportion of each component was calculated across all sampled paraffin blocks. In contrast, for prognosis analysis, the overall tumor component ratio was calculated by summing the total amounts of each component across all lesions and dividing by the total amount of all tumors.

Statistical Analysis

SPSS (version 25.0; IBM, Armonk, NY) and MedCalc® Statistical Software (version 20; Ostend, Belgium; 2021) were used for all statistical analyses. Quantitative data following a normal distribution are presented as mean ± standard deviation, while abnormally distributed data are expressed as medians and inter-quartile ranges. Pearson or Spearman correlation analysis was used to assess the relationship between the TEVR and the pathological proportions of viable tumor cells, tumor stroma, and non-necrotic tissue (the sum of viable tumor and tumor stroma). The ratio of viable tumor cells (RVTCs) was then correlated with recurrence-free survival time using ROC curve analysis to identify the optimal cutoff value, which was defined as MPR. ROC curve analysis was performed to evaluate the diagnostic performance of TEVR from the AI software in identifying MPR and to determine the threshold value. Survival curves were generated using the Kaplan–Meier method and compared with the Log rank test. Univariable and multivariable Cox regression models were used to identify independent prognostic factors for RFS after conversion surgery following HAIC-TI in

https://doi.org/10.2147/JHC.S527789

uHCC patients. Interobserver agreement for imaging-based treatment response assessments was evaluated using the Cohen's κ statistic. A two-sided $p < 0.05$ was considered statistically significant.

Results

Clinical Characteristics, Treatment Response, and Follow-Up

One patient was excluded due to segmentation failure, as the tumor extended beyond the hepatic contour, leading to inaccurate delineation by the automated algorithm. Finally, 35 patients with 46 lesions were included in the analysis (Table 1). All patients underwent HAIC-TI, with 4 having previously received TACE before HAIC treatment. The median number of HAIC treatment cycles was 3 (IQR: 2–5.5 cycles). The median interval between baseline and the final preoperative MRI examination was 4 months (IQR: 2–6 months).

According to the mRECIST criteria, there were 8 cases of SD, 19 cases of PR, 6 cases of CR, and 2 case of PD. The one-dimensional measurements of the maximum diameter of each lesion and the enhancing portion based on mRECIST criteria were summarized in Table 2. Regarding interobserver agreement, mRECIST-based response evaluation demonstrated moderate to good consistency, with a κ value of 0.739 (95% CI: 0.527–0.951, $P < 0.001$), as shown in Table 3.

The median RFS for intrahepatic and extrahepatic recurrence was 23 months and 20 months, respectively. Postoperatively, 11 patients had recurrence confined to the liver, 3 patients died, and 4 patients had recurrence limited to extrahepatic sites. Only one patient did not receive adjuvant therapy due to impaired liver function, while the remaining 34 patients received various types of adjuvant therapies, including targeted therapy, immunotherapy, combination therapy with targeted therapy and immunotherapy, or additional HAIC.

Table 1 Patients Characteristics

Parameter	Number (n = 35)
Age, years	55.00 (IQR: 52.00–64.50)
Male	33 (94.3)
Underlying liver disease	
HBV	35 (100.0)
Cirrhosis	31 (88.6)
Child-Pugh A	31 (88.6)
Child-Pugh B	4 (11.4)
BCLC stage	
A-B	20 (57.1)
C	15 (42.9)
Preoperative serum AFP > 400 ng/mL	8 (22.9)
Preoperative serum AFP > 100 ng/mL	12 (35.3)
Total number of lesions on preoperative MRI	
1	27 (77.1)
2	5(14.3)
3	3 (8.6)
Baseline tumor diameter (mm)	84.1 (IQR: 41–116)
Preoperative tumor diameter (mm)	43.0 (IQR: 21–83)
Preoperative tumor diameter ≥ 30 mm	29 (63)
Postoperative Treatment	
No Treatment	1 (2.9)
Maintenance Chemotherapy	17 (48.6)
HAIC	9 (25.7)
HAIC-TI	8 (22.9)

Note. Data are number of patients; data in parentheses are percentages.
Abbreviations: IQR, interquartile range; HBV, hepatitis B virus; BCLC, Barcelona Clinic Liver Cancer; AFP, alpha-fetoprotein, HAIC-TI, hepatic arterial infusion chemotherapy combined with targeted therapy and immunotherapy.

Table 2 One-Dimensional Measurements of HCC Lesions

Variable	Baseline MRI	Final Preoperative MRI
Maximum diameter of each lesion (mm)	84.5 (IQR: 41.0–116.0)	47.0 (IQR: 21.8–84.0)
Maximum diameter of target lesion (mRECIST) (mm)	103.0 (IQR: 72.0–120.0)	36.0 (IQR: 16.0–62.0)

Abbreviations: HCC, hepatocellular carcinoma; RECIST, modified response evaluation criteria in solid tumors; IQR, interquartile range.

Table 3 Interobserver Agreement for Imaging-Based Assessments of Treatment Response

MRI Response Evaluation Criteria	κ Value (95% CI)	*P* Value
mRECIST	0.739 (0.527, 0.951)	<0.001

Abbreviations: mRECIST, modify response evaluation criteria in solid tumors, CI, Confidence Interval.

Pathologic Findings

Among the 46 lesions, 17 (37.0%) achieved pCR, while at the patient level (n = 35), 11 (31.4%) achieved pCR. Pathologic examination demonstrated varying degrees of tumor necrosis and stromal components across all lesions (Table 4). Additionally, microvascular invasion (MVI) was detected in 8 lesions (17.4%), while no viable tumor cells were found in tumor thrombi.

AI-Based Automated MRI Tumor and Enhancement Volume

The AI-generated segmentation and quantification of tumor volume, intratumoral enhancement volume, and the TEVR were presented in Table 5.

Correlation Between AI-Quantified Enhancement Volume Ratio and Pathological Tissue Proportions

The TEVR during the portal venous phase exhibited a strong correlation with the non-necrotic tissue ratio (viable tumor cells + tumor stroma) ($r = 0.89$, $p < 0.001$), better than the arterial phase ($r = 0.79$, $p < 0.001$); both of them showed moderate correlation

Table 4 Summary of Pathologic Findings at the Per-Lesion and Per-Patient Levels

Variable	Per-Lesion (n = 46)	Per-Patient (n = 35)
Median viable tumor proportion (%) (IQR)	10 (0–40)	10 (0–40)
Median tumor stroma proportion (%) (IQR)	20 (10–35)	27.5 (15–45)
Median non-necrotic tissue proportion (%) (IQR)	37.5 (25–75)	45 (25–70)
Median necrotic proportion (%) (IQR)	62.5 (25–75)	47.5 (15–75)

Abbreviations: pCR, pathological complete response; IQR, interquartile range.

Table 5 AI-Based Quantification of Tumor Volume, Intratumoral Enhancement Volume, and Tumor Enhancement Volume Ratio

Variable	Per-Lesion	Total Tumor Burden
Tumor Volume (cm^3) (IQR)	83.0 (27.2–233.5)	83.4 (34.5–233.5)
Arterial Phase Enhancement Volume (cm^3) (IQR)	43.0 (6.9–103.6)	43.24 (12.2–103.6)
Arterial Phase Enhancement Ratio (%) (IQR)	52.9 (36.7–71.1)	51.9 (29.3–71.1)
Portal Venous Phase Enhancement Volume (cm^3) (IQR)	10.0 (4.00–55.7)	10.0 (3.5–55.7)
Portal Venous Phase Enhancement Ratio (%) (IQR)	21.8 (7.9–54.2)	16.4 (6.2–45.3)

Abbreviation: IQR, interquartile range.

with the viable tumor ratio and the tumor stroma ratio. The scatter plots and residual plots depicting the correlation between the TEVR at various MRI phases and the pathological component proportions were shown in Figures 2a–f and 3a–f. The comparison between imaging findings, gross specimens, and pathological section images was shown in Figure 4.

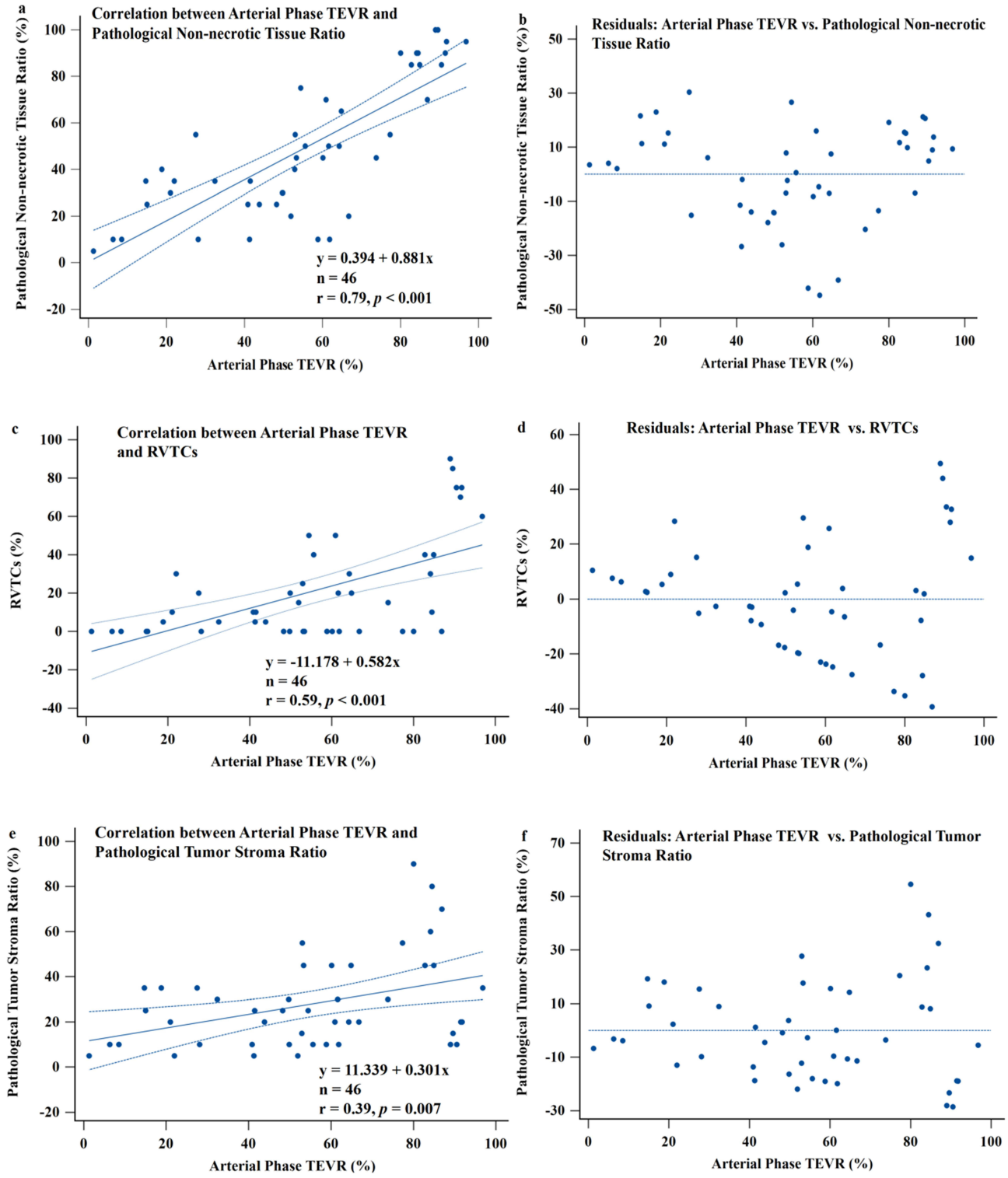

Figure 2 (**a–f**) showed the correlation and residual plots between the AI-quantified MRI arterial phase enhancement volume ratio and the pathological non-necrotic tissue ratio (viable tumor + tumor stroma), viable tumor cell ratio, and tumor stroma ratio, respectively.

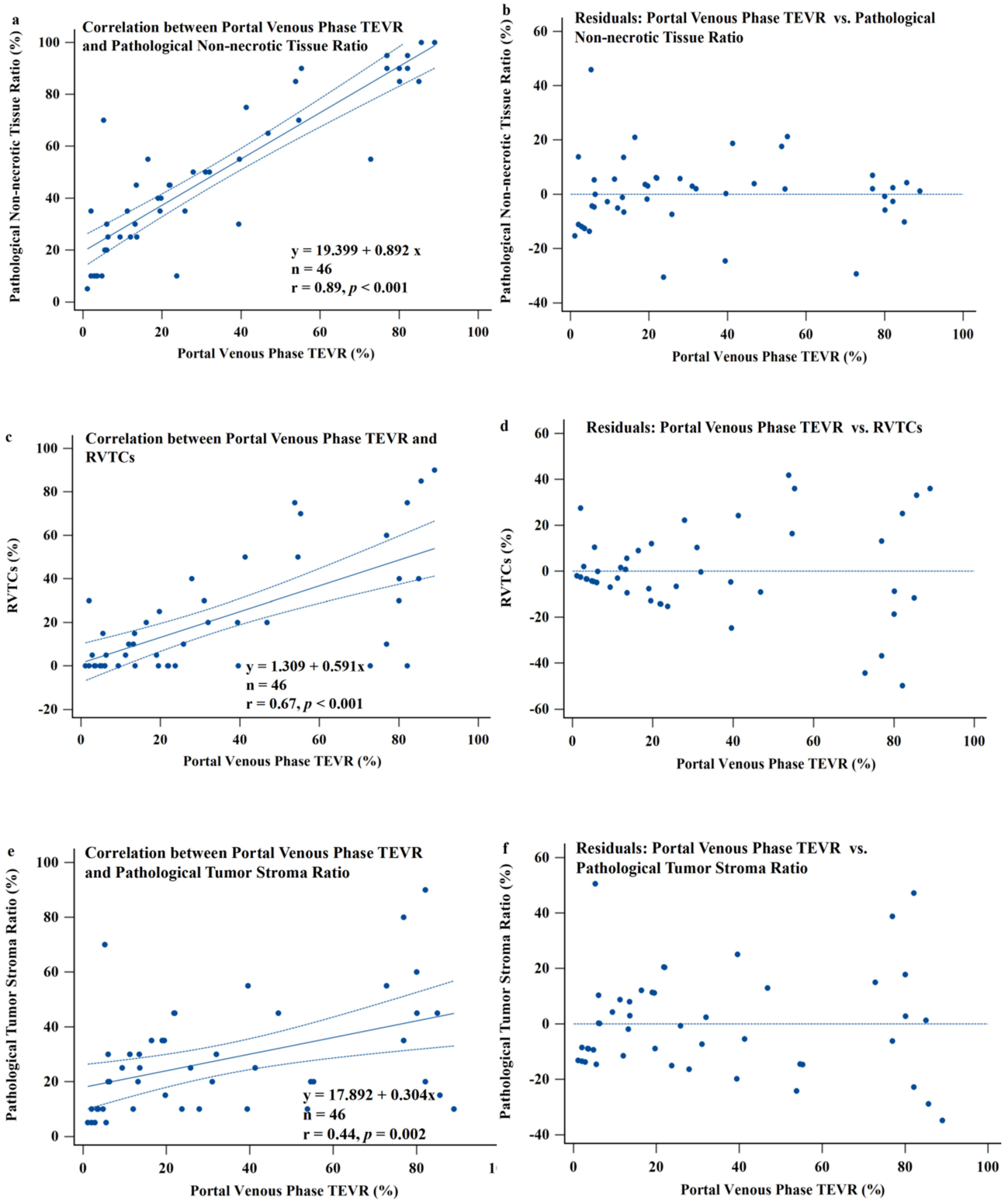

Figure 3 (**a**–**f**) showed the correlation and residual plots between the AI-quantified MRI portal venous phase enhancement volume ratio and the pathological non-necrotic tissue ratio (viable tumor + tumor stroma), viable tumor cell ratio, and tumor stroma ratio, respectively.

https://doi.org/10.2147/JHC.S527789

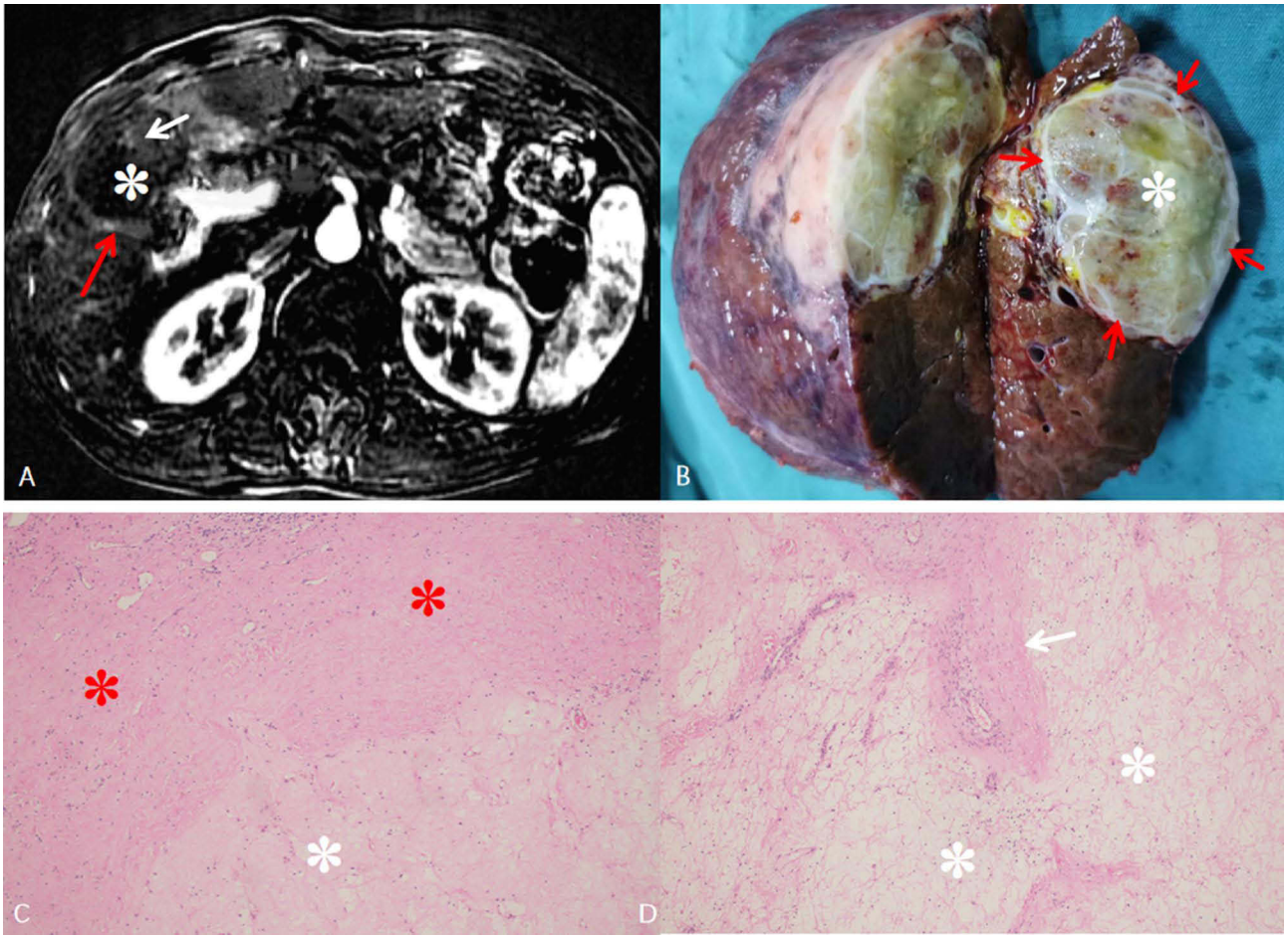

Figure 4 Representative images of a 52-year-old man comparing radiographic and pathological response evaluations. The patient underwent surgical resection 6 months after six cycles of hepatic artery infusion chemotherapy combined with targeted therapy and immunotherapy, with postoperative pathology confirming a complete response. Axial T1-weighted arterial phase image (**A**) showed a 65 mm hepatocellular carcinoma (*) in segment V, featuring a peripheral enhancing capsule sign (long red arrow), central necrosis (white *), and an enhancing focus within the lesion (white arrow). The gross specimen photograph (**B**) revealed an intact white fibrous capsule at the lesion margin (short red arrow) and intralesional necrosis (white *). Pathological comparison images (**C** and **D**) of the lesion (original magnification × 100, and × 100, respectively; hematoxylin-eosin staining) showed fibrous connective tissue (red *) at the lesion periphery and intralesional necrosis (white *). D highlights tumor stroma (fibrous and inflammatory cells) (white arrow) in the central area of the lesion, corresponding to the enhancing area in image A, along with intralesional necrosis (white *).

Prognostic Significance of the Ratio of Viable Tumor Cells in Postoperative Intrahepatic Recurrence

ROC curve analysis identified RVTCs ≤ 10% as the optimal cutoff value for predicting postoperative intrahepatic recurrence, with an area under the curve (AUC) of 0.808 ($p < 0.001$). Based on this cutoff value, MPR was defined as RVTCs ≤ 10%. Eighteen patients achieved MPR.

Diagnostic Performance of AI-Based MRI Enhancement Volume Ratio in Evaluating MPR

ROC curve analysis demonstrated that the portal venous phase TEVR exhibited superior diagnostic performance for MPR compared to the arterial phase, with an AUC of 0.879 ($p < 0.001$) vs 0.703 ($p = 0.026$). The optimal cutoff values for MPR diagnosis were TEVR ≤ 19.5% in the portal venous phase and TEVR ≤ 49.7% in the arterial phase. At these cutoff values, the sensitivity and specificity of TEVR in the portal venous phase were 88.89% and 82.35%, respectively, whereas those in the arterial phase were 66.67% and 76.47%, respectively (Figure 5).

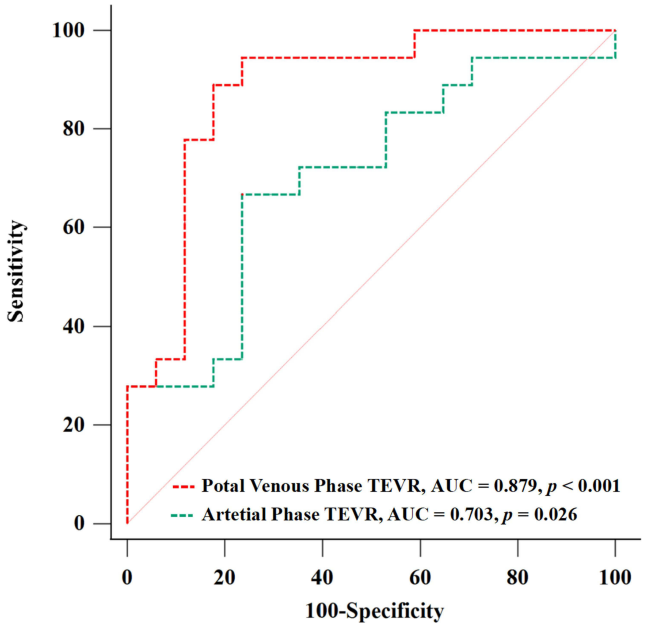

Figure 5 Receiver operating characteristic (ROC) curve analysis of the tumor enhancement volume ratio (TEVR) in the arterial phase and portal venous phase for diagnosing pathological major partial response (pMPR). The optimal cutoff values were TEVR > 49.7% in the arterial phase and TEVR > 19.5% in the portal venous phase. The corresponding area under the curve (AUC) values were 0.703 (p = 0.026) and 0.812 (p < 0.001), respectively.

Prognostic and Predictive Analysis of Postoperative Intrahepatic Recurrence

The results of Kaplan–Meier (KM) survival analysis were presented in Figure 6a–f. KM survival analysis demonstrated that patients with MPR (RVTCs ≤ 10%) had significantly longer RFS (median survival time: not reached) compared to those with non-MPR (RVTCs > 10%) (median survival time: 11.0 months) (p = 0.004). Patients with CR and MVI^{-} had significantly longer RFS (p = 0.019, p = 0.013, respectively).

According to mRECIST criteria, a significant difference in RFS was observed among response group (median survival time: not reached), and non-response group (median survival time: 11.0 months), (p = 0.024).

For AI-based MRI quantification, the portal venous phase TEVR demonstrated significant prognostic value, with patients having TEVR ≤ 19.5% exhibiting significantly prolonged RFS (median survival time: not reached) compared to those with TEVR > 19.5% (median survival time: 11.0 months) (p = 0.035). However, the arterial phase TEVR did not show a significant association with RFS (p = 0.714).

The results of univariable and multivariable Cox regression analyses were summarized in Table 6.

Only MPR (RVTCs ≤ 10%) showed significantly associated with RFS in both univariable and multivariable analyses of Model 1 (including pathology, imaging and clinical indicators) (HR = 0.19, 95% CI: 0.05–0.69, p = 0.011). MVI^{+} showed significance in univariable analysis (HR = 0.19, 95% CI: 3.29 (1.19–9.09), p = 0.022) but was not retained in Model 1.

Portal venous phase TEVR (≤19.5%) was significantly associated with RFS in univariable analysis (HR = 0.33, 95% CI: 0.012–1.00, p = 0.049) and Model 2 (including imaging and clinical indicators) (p = 0.049). mRECIST showed significance in univariable analysis (p = 0.024) but was not retained in Model 2.

Arterial phase TEVR (≤49.7%), AFP levels (>100 ng/mL and >400 ng/mL), BCLC stage, tumor size, tumor number, Child-Pugh score, preoperative HAIC treatment cycles, and postoperative treatment status were also not significantly associated with RFS (all p > 0.05).

https://doi.org/10.2147/JHC.S527789

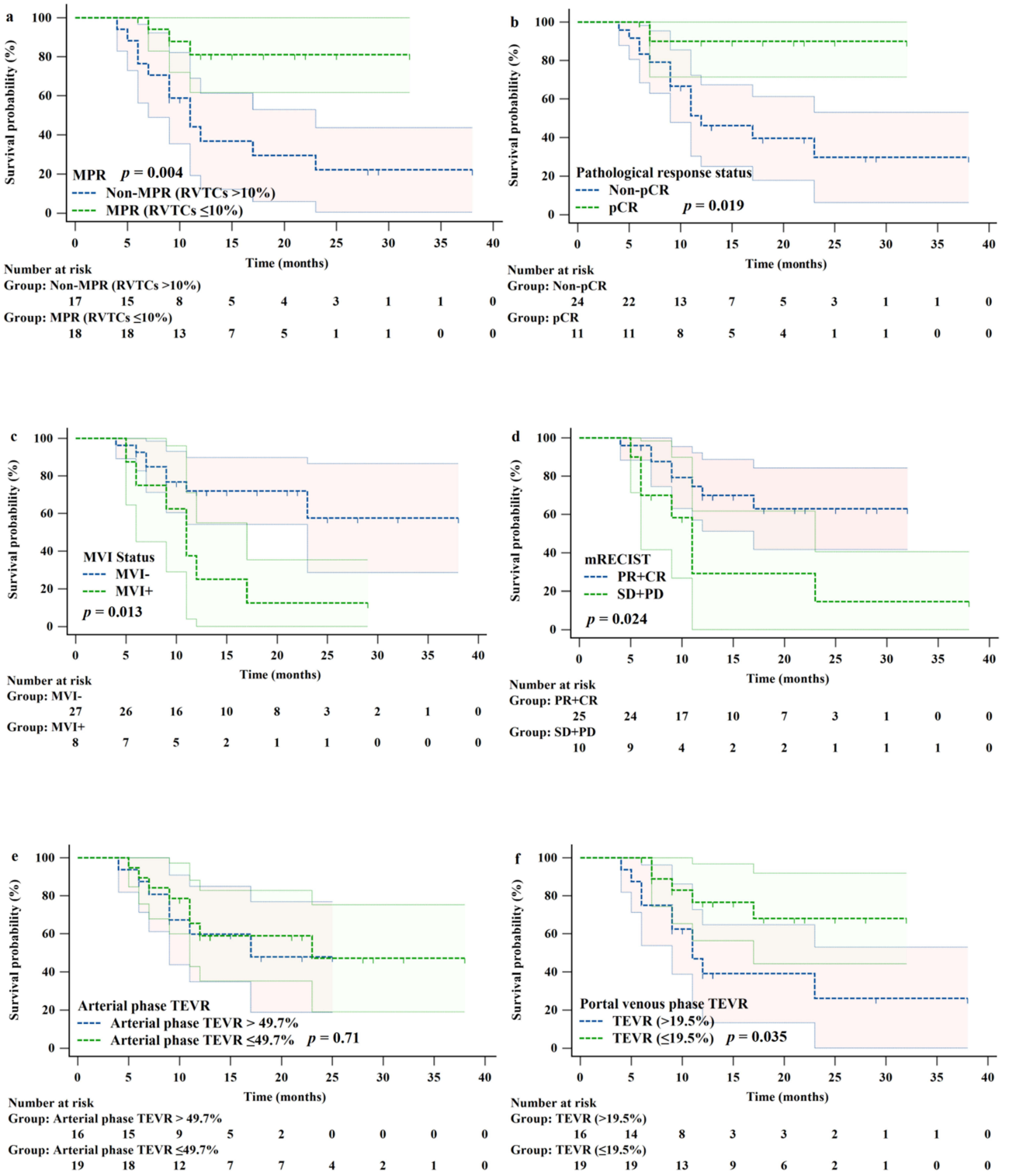

Figure 6 (**a**–**f**) Kaplan–Meier survival curves for postoperative intrahepatic recurrence stratified by different prognostic factors. (**a**) Major pathological response (MPR): Patients with MPR (the ratio of viable tumor cells, RVTCs ≤ 10%) had significantly better recurrence-free survival (RFS) compared to those with Non-MPR (RVTCs > 10%) (p = 0.004). (**b**) Pathological response status: A significant difference in RFS was observed among patients classified as complete response (CR) and partial response (PR) (p = 0.019). (**c**) Microvascular invasion (MVI) status: A significant difference in RFS was observed among patients classified as MVI- and MVI+ (p = 0.013). (**d**) mRECIST criteria: Patients achieving PR or CR had significantly improved RFS compared to those with SD or PD (p = 0.024). (**e**) Arterial phase tumor enhancement volume ratio (TEVR) stratification: No significant difference in RFS was observed between patients with TEVR ≤ 49.7% and TEVR > 49.7% (p = 0.710). (**f**) Portal venous phase TEVR stratification: Patients with TEVR ≤ 19.5% had significantly prolonged RFS compared to those with TEVR > 19.5% (p = 0.035).

Table 6 Univariable and Multivariable Cox Regression Analysis for Predicting Postoperative Intrahepatic Recurrence

Variable	Univariable		Multivariable: Model 1*		Multivariable: Model 2*	
	HR (95% CI)	*P* Value	HR (95% CI)	*P* Value	HR (95% CI)	*P* Value
Pathologic Factors						
MPR (RVTCs ≤ 10%)	0.19 (0.05–0.69)	0.011	0.19 (0.05–0.69)	0.011		
pCR	0.13 (0.02–1.00)	0.052				
MVI^+	3.29 (1.19–9.09)	0.02				
Imaging Factors						
Arterial Phase TEVR (≤49.7%)	0.83 (0.30–2.31)	0.72				
Portal Venous Phase TEVR (≤19.5%)	0.34 (0.12–1.00)	0.049			0.34 (0.12–1.00)	0.049
mRECIST	3.01 (1.08–8.41)	0.036				
Clinical Variables						
AFP (>100ng/mL)	1.23 (0.44–3.45)	0.70				
AFP (>400ng/mL)	0.81 (0.23–2.89)	0.75				
BCLC Stage (A/B vs C)	1.18 (0.66–2.11)	0.57				
Number of Tumors	1.88 (0.96–3.70)	0.07				
Child-Pugh Score	1.70 (0.38–7.68)	0.49				
Tumor Size (≥5 cm)	0.84 (0.30–2.32)	0.74				
Tumor Size (≥3cm)	1.26 (0.29–5.60)	0.76				
Preoperative HAIC-TI Treatment Cycles	1.24 (0.93–1.66)	0.14				
Postoperative Treatment Status	1.22 (0.66–2.25)	0.53				

Notes: *Model 1 included pathological, imaging, and clinical variables, whereas Model 2 excluded pathological variables and assessed only imaging and clinical factors.

Abbreviations: HR, hazard ratio; CI, confidence interval; MPR, major pathological response; pCR, pathological complete response; RVTCs, ratio of viable tumor cells; TEVR, tumor enhancement volume ratio; mRECIST, modified response evaluation criteria in solid tumors; AFP, alpha-fetoprotein; BCLC, Barcelona Clinic Liver Cancer; MVI, microvascular invasion; HAIC-TI, hepatic arterial infusion chemotherapy combined with targeted therapy and immunotherapy.

Discussion

MPR (RVTCs ≤ 10%) is an established prognostic marker in lung cancer after neoadjuvant therapy,[32] but no consensus exists on the RVTCs threshold for defining MPR in HCC.[9] Some studies have reported that uHCC patients achieving pCR after conversion therapy exhibit significantly improved RFS.[9,14,23] In our study, KM survival analysis demonstrated that patients with pCR had significantly longer RFS ($p = 0.019$), as previously reported.[23] However, pCR did not reach statistical significance in univariable COX analysis ($p = 0.052$) and was not retained in Model 1. The lack of statistical significance for pCR in multivariable analysis may be due to its strict definition, where even minimal residual tumor leads to classification as non-pCR. This binary distinction may not adequately capture the prognostic continuum, unlike MPR which includes patients with low but non-zero residual viable tumor. In contrast, MPR was significantly associated with prolonged RFS ($p = 0.004$) and remained an independent predictor in multivariable Cox regression analysis (HR = 0.19, $p = 0.011$). We speculate that, in addition to patients achieving pCR, those with minimal residual viable tumor were also associated with longer RFS. Therefore, MPR, by encompassing a wider range of meaningful pathological responses, may provide a more comprehensive and potentially superior surrogate to pCR for predicting recurrence risk following HAIC-TI.

The AI software used in this study (LiverMRDoc) is a commercially available tool based on deep learning–driven 3D U-Net algorithms. Although we did not independently assess its segmentation performance in this study, the same software and underlying algorithm have previously been validated in patients with HCC. One study demonstrated its high segmentation efficiency and reproducibility in portal venous phase imaging, achieving a mean Dice similarity coefficient (DSC) of 0.902 for Couinaud liver segments, with a processing time of only 8 seconds per case.[29] In another study involving 35 randomly selected patients with 40 HCCs, one radiologist manually segmented the tumors using ITK-SNAP (version 3.8.0), while blinded to the automated results. The comparison showed a high level of agreement between automated and manual segmentations, with a mean DSC of 0.85 ± 0.11 (median: 0.88; IQR: 0.82–0.92) across MRI sequences.[31] These findings support the technical robustness and reliability of this AI platform for volumetric tumor

analysis in HCC. Building upon this platform, our findings demonstrated that AI-quantified TEVR had a strong correlation with pathological components, particularly in the portal venous phase (r = 0.89, $p < 0.001$), supporting the value of AI-based imaging in assessing pathological response in uHCC. Portal venous phase TEVR (≤19.5%) also demonstrated superior diagnostic performance for identifying MPR (AUC = 0.879) compared to the arterial phase (AUC = 0.703). Furthermore, it was significantly associated with RFS in univariable analysis (HR = 0.33, $p = 0.049$) and retained significance in a multivariable model incorporating clinical and imaging parameters ($p = 0.049$), suggesting its potential as an imaging-based prognostic biomarker. However, when pathological variables such as MPR and MVI were included in the model 1, only MPR remained statistically significant. This may be partially explained by the limited sample size (n = 35), which could reduce statistical power in models involving multiple interrelated predictors. In addition, because MPR represents a pathological gold standard for assessing treatment response, the prognostic contribution of TEVR—an imaging surrogate partially overlapping with MPR—may have been attenuated in this context. Notably, in a separate model excluding pathological variables, portal venous phase TEVR (≤19.5%) remained a significant independent predictor of RFS. This finding reinforces its clinical utility in settings where pathological assessment is unavailable, such as in non-surgical patients or preoperative decision-making. While MPR remains the definitive endpoint for pathological confirmation, TEVR may serve as a practical, reproducible, and fully automated imaging marker to support real-world clinical decision-making in the management of uHCC.

Although mRECIST is currently used as the most commonly used imaging tumor response assessment after HCC conversion therapy,[10,14,15,18,24,25] it is not an independent predictor of RFS and only showed statistically different in the univariable Cox regression analyses ($p = 0.024$). This may be related to that mRECIST assesses efficacy response in terms of the proportion of change in the viable tumor. Specifically, PR is defined as a ≥30% reduction in the longest diameter of enhancing tumor tissue,[24,25] which encompasses a wide spectrum of residual tumor sizes and may weaken its specificity in prognostication. Moreover, mRECIST relies on one-dimensional, manual measurements that are inherently subjective and prone to interobserver variability. It also typically requires longitudinal follow-up to assess temporal changes in enhancement,[24,25] which may delay clinical decision-making. According to mRECIST guidelines, only up to two target lesions per organ are quantitatively assessed, while non-target lesions are evaluated qualitatively.[24,25] In advanced-stage uHCC, where multiple intrahepatic lesions are common, this selective measurement strategy may not fully reflect the overall tumor burden or therapeutic response. In contrast, the AI-based quantitative method evaluates tumor burden from a single preoperative MRI scan, enabling timely assessment without the need for serial imaging. TEVR, automatically calculated using a 3D U-Net–based DL algorithm, demonstrated excellent diagnostic performance for predicting MPR (AUC = 0.879). In addition, the AI workflow is fully automated and highly efficient, with segmentation completed in approximately 8 seconds per case—substantially faster than manual annotation.[29] Furthermore, AI volumetric analysis captures the entire 3D enhancement profile of all lesions, including irregular or multifocal enhancement patterns and those deemed non-target by mRECIST, thereby offering a comprehensive and reproducible measure of residual viable tumor burden. These features reduce operator dependence, improve reproducibility, and may offer a more objective and clinically practical alternative to traditional response criteria in evaluating uHCC after HAIC-TI.

Following HAIC-TI, imaging-based assessment of residual viable tumor using contrast enhancement can be substantially confounded by the presence of tumor stroma. In our cohort, uHCC lesions exhibited a median stromal component of 20% (IQR: 10–35%), comprising predominantly inflammatory cells, vasculature, and fibrotic tissue. These non-viable yet enhancing components often exhibit irregular morphologies on contrast-enhanced MRI, mimicking viable tumor tissue. This phenomenon has been described in previous study,[32] and may lead to systematic overestimation of residual viable tumor burden by enhancement-based imaging techniques. This pathological overlap likely underlies the observed discrepancy in correlation strengths: while portal venous phase TEVR showed a strong correlation with the proportion of non-necrotic tissue (viable tumor cells + tumor stroma) (r = 0.89, $p < 0.001$), its correlation with RVTCs alone was moderate (r = 0.67, $p < 0.001$). This suggests that portal venous phase TEVR, although sensitive to enhancing tissue, cannot fully distinguish between biologically active tumor and inactive stromal components. Despite this limitation, the prognostic utility of TEVR remains robust. Stromal tissues—being non-proliferative and biologically inert—may have limited influence on recurrence risk, particularly in the context of large tumor burdens (median tumor size: 62.0 mm, IQR: 45.0–91.0 mm) in our study. Therefore, portal venous phase TEVR may be better interpreted as a surrogate marker for non-necrotic tissue volume rather than residual viable tumor alone, and still retain predictive value for RFS. To improve biological specificity, multiparametric MRI techniques such as diffusion-weighted imaging

(DWI) and ADC mapping can offer important complementary information. Diffusion restriction reflects increased cellular density, a hallmark of viable tumor tissue, whereas fibrotic or necrotic regions typically demonstrate less restricted diffusion. Consequently, DWI-derived parameters may help distinguish viable tumor from non-viable stromal components that also exhibit contrast enhancement. A prior study has demonstrated that integrating enhancement-based and ADC-based volumetric analysis markedly improved the correlation with histopathologic necrosis compared to conventional visual assessment alone ($R^2 = 0.9662$ for qADC; residual standard error ≈ 6.3%).[27] These findings underscore the potential of combining structural and functional imaging features to improve the specificity and accuracy of response evaluation, particularly in complex post-treatment tumor environments. Although the AI algorithm used in our study operated exclusively on contrast-enhanced MRI sequences and did not incorporate DWI or ADC inputs, our findings indicate that stromal components may contribute to overestimation of viable tumor burden. This limitation suggests that integrating DWI-based parameters into future AI models may enhance their ability to distinguish biologically active from inactive enhancing tissue. Prospective studies incorporating multiparametric imaging inputs may further refine the precision and clinical utility of automated tumor response assessments in uHCC.

We further compared the diagnostic performance of arterial and portal venous phase TEVR in predicting pathological response. Although HAIC-TI substantially reduces arterial perfusion to the tumor,[18] residual inflammatory activity, stromal proliferation, or reparative neovascularization may still produce nonspecific enhancement during the arterial phase. These non-tumoral enhancing components—often characterized by irregular morphology—can be inadvertently interpreted as residual viable tumor by automated algorithms, resulting in overestimation of arterial phase TEVR. So, arterial phase algorithms should be optimized in the future. In our ROC analysis, the optimal cutoff for arterial phase TEVR was 49.7%, markedly higher than that for the portal venous phase (19.5%). This elevated threshold likely reflects the need to filter out false-positive enhancement caused by non-tumoral tissue, as only a large extent of arterial enhancement may indicate residual viable tumor. Nonetheless, the diagnostic performance of arterial phase TEVR remained limited (AUC = 0.703; sensitivity = 66.67%), potentially due to both therapy-induced tumor hypovascularity and confounding enhancement from non-tumoral tissue. In contrast, portal venous phase enhancement is more sustained and less susceptible to transient stromal or inflammatory changes. Even at a lower threshold, portal venous phase TEVR demonstrated superior diagnostic performance for identifying MPR (AUC = 0.879), with higher sensitivity (88.89%) and specificity (82.35%). These findings support the utility of portal venous phase TEVR as a more reliable imaging biomarker for treatment response. Notably, this aligns with the CT/MRI Liver Imaging Reporting and Data System Treatment Response Assessment algorithm (version 2024),[33] which recognizes that radiologic viability can be manifested in any contrast phase, not limited to the arterial phase. The superior performance of portal-phase TEVR observed in our study is consistent with this principle, as it better captures the persistent enhancement patterns characteristic of viable tumor.

This study has several limitations. First, the relatively small sample size (n = 35) and single-center retrospective design may limit statistical power, had selection bais and reduce the generalizability of the findings. In addition, no independent validation cohort was included. Moreover, intrahepatic recurrence, rather than OS, was used as the primary endpoint, which may not fully reflect clinical outcomes. Second, although AI-based segmentation was utilized and preoperative MRI findings were reviewed by MDT to guide pathological sampling, perfect spatial concordance between imaging and pathology remains difficult to achieve. Furthermore, the estimation of histological components was performed by visual assessment in 5% increments, which may introduce observer variability. Future studies should consider incorporating digital pathology or other quantitative histologic analysis techniques to improve accuracy and reproducibility. Third, the AI algorithm in this study primarily quantified enhancement volume. However, following HAIC-TI, tumor stroma may also enhance due to inflammatory or fibrotic changes, complicating the differentiation from residual viable tumor. Additionally, variations in HAIC-TI treatment protocols may have contributed to heterogeneity in imaging findings and pathological outcomes. Incorporating additional imaging sequences such as diffusion-weighted imaging (DWI) and refining algorithms to account for stromal characteristics may improve diagnostic specificity. Future research should prioritize external validation using larger, prospectively collected, multi-center datasets, and explore the integration of multiparametric MRI with advanced AI models and quantitative pathology to enhance the clinical applicability and robustness of imaging-based response assessment in uHCC.

In conclusion, portal venous phase TEVR derived from AI-based MRI quantification demonstrated a strong correlation with pathological components and provided superior diagnostic accuracy for MPR, as well as significant prognostic

value for RFS. Integrating AI-based volumetric assessment into clinical workflows may improve treatment monitoring, guide surgical timing following HAIC-TI, and optimize post-surgical management.

Critical Relevance Statement

AI-based quantitative MRI assessment on portal venous phase after HAIC-TI conversion therapy can effectively correlated with pathological response and associated with RFS, and it can assist in clinical therapeutic decision-making, especially for the timing of surgery.

Abbreviations

HCC, hepatocellular carcinoma; HAIC-TI, hepatic arterial infusion chemotherapy plus targeted therapy and immunotherapy; Mrecist, modified response evaluation criteria in solid tumors; pCR, pathologic complete response; MPR, major pathological response; AI, artificial intelligence.

Data Sharing Statement

The datasets used and/or analyzed during the current study are available from the corresponding author (liuziyu301@163.com) on reasonable request.

Ethical Approval

The protocol of this retrospective study conformed to the Declaration of Helsinki (1975) and its amendments and was approved by the Ethics Review Committee of the First Affiliated Hospital of Chongqing Medical University (2025-338-01), which waived the requirement for written informed consent because patients or their legal guardians had consented, upon admission, to analysis and publication of anonymized medical data for research purposes.

Acknowledgments

This work was supported by Program for Youth Innovation in Future Medicine, Chongqing Medical University (No: W0096).

Funding

This work was supported by Program for Youth Innovation in Future Medicine, Chongqing Medical University (No: W0096).

Disclosure

The authors declared that they have no conflicts of interest in this work.

References

1. Sung H, Ferlay J, Siegel RL, et al. Global cancer statistics 2020: GLOBOCAN estimates of incidence and mortality worldwide for 36 cancers in 185 countries. *CA a Cancer J Clin*. 2021;71(3):209–249. doi:10.3322/caac.21660
2. Park J, Chen M, Colombo M, et al. Global patterns of hepatocellular carcinoma management from diagnosis to death: the BRIDGE study. *Liver Inter*. 2015;35(9):2155–2166. doi:10.1111/liv.12818
3. Llovet JM, Kelley RK, Villanueva A, et al. Hepatocellular carcinoma. *Nat Rev Dis Primers*. 2021;7(1):6. doi:10.1038/s41572-020-00240-3
4. Chen QF, Chen S, Chen M, Lyu N, Zhao M. Improving the conversion success rate of hepatocellular carcinoma: focus on the use of combination therapy with a high objective response rate. *J Clin Transl Hepatol*. 2024. doi:10.14218/JCTH.2023.00403
5. Sangro B, Sarobe P, Hervás-Stubbs S, Melero I. Advances in immunotherapy for hepatocellular carcinoma. *Nat Rev Gastroenterol Hepatol*. 2021;18(8):525–543. doi:10.1038/s41575-021-00438-0
6. Memeo R, Pisani AR, Ammendola M, de'Angelis N, Inchingolo R. A new era for hepatocellular carcinoma. *Hepatobiliary Surg Nutr*. 2023;12(1):135–136. doi:10.21037/hbsn-23-10
7. Kudo M, Finn RS, Galle PR, et al. IMbrave150: efficacy and safety of atezolizumab plus bevacizumab versus sorafenib in patients with Barcelona clinic liver cancer stage B unresectable hepatocellular carcinoma: an exploratory analysis of the Phase III study. *Liver Cancer*. 2023;12(3):238–250. doi:10.1159/000528272
8. Ho WJ, Zhu Q, Durham J, et al. Neoadjuvant cabozantinib and nivolumab convert locally advanced hepatocellular carcinoma into resectable disease with enhanced antitumor immunity. *Nat Cancer*. 2021;2(9):891–903. doi:10.1038/s43018-021-00234-4

9. Sun HC, Zhou J, Wang Z, et al. Alliance of Liver Cancer Conversion Therapy, Committee of Liver Cancer of the Chinese Anti-Cancer Association. Chinese expert consensus on conversion therapy for hepatocellular carcinoma (2021 edition). *Hepatobiliary Surg Nutr*. 2022;11(2):227–252. doi:10.21037/hbsn-21-328.
10. Kudo M, Kawamura Y, Hasegawa K, et al. Management of hepatocellular carcinoma in Japan: JSH consensus statements and recommendations 2021 update. *Liver Cancer*. 2021;10(3):181–223. doi:10.1159/000514174
11. Hendi M, Mou Y, Lv J, Zhang B, Cai X. Hepatic arterial infusion chemotherapy is a feasible treatment option for hepatocellular carcinoma: a new update. *Gastrointest Tumors*. 2021;8(4):145–152. doi:10.1159/000516405
12. Zheng K, Zhu X, Fu S, et al. Sorafenib plus hepatic arterial infusion chemotherapy versus sorafenib for hepatocellular carcinoma with major portal vein tumor thrombosis: a randomized trial. *Radiology*. 2022;303(2):455–464. doi:10.1148/radiol.211545
13. Chen CT, Liu TH, Shao YY, Liu KL, Liang PC, Lin ZZ. Revisiting hepatic artery infusion chemotherapy in the treatment of advanced hepatocellular carcinoma. *IJMS*. 2021;22(23):12880. doi:10.3390/ijms222312880
14. Yu B, Zhang N, Feng Y, Zhang Y, Zhang T, Wang L. Hepatectomy after conversion therapy with hepatic arterial infusion chemotherapy, tyrosine kinase inhibitors and anti-PD-1 antibodies for initially unresectable hepatocellular carcinoma. *JHC*. 2023;10:1709–1721. doi:10.2147/JHC.S432062
15. Chen CB, Chen CM, Tzeng RH, et al. Combining HAIC and sorafenib as a salvage treatment for patients with treatment-failed or advanced hepatocellular carcinoma: a single-center experience. *JCM*. 2023;12(5):1887. doi:10.3390/jcm12051887
16. Zhou H, Song T. Conversion therapy and maintenance therapy for primary hepatocellular carcinoma. *BST*. 2021;15(3):155–160. doi:10.5582/bst.2021.01091
17. Yao W, Wei R, Jia J, et al. Development and validation of prognostic nomograms for large hepatocellular carcinoma after HAIC. *Ther Adv Med Oncol*. 2023;15:175883592311638. doi:10.1177/17588359231163845
18. Li Y, Liu W, Chen J, et al. Efficiency and safety of hepatic arterial infusion chemotherapy (HAIC) combined with anti- PD1 therapy versus HAIC monotherapy for advanced hepatocellular carcinoma: a multicenter propensity score matching analysis. *Cancer Medicine*. 2024;13(1):e6836. doi:10.1002/cam4.6836
19. Liu D, Mu H, Liu C, et al. Sintilimab, bevacizumab biosimilar, and HAIC for unresectable hepatocellular carcinoma conversion therapy: a prospective, single-arm Phase II trial. *neo*. 2024;70(06):811–818. doi:10.4149/neo_2023_230806N413
20. Zhu XD, Huang C, Shen YH, et al. Downstaging and resection of initially unresectable hepatocellular carcinoma with tyrosine kinase inhibitor and anti-PD-1 antibody combinations. *Liver Cancer*. 2021;10(4):320–329. doi:10.1159/000514313
21. Habibollahi P, Shamchi SP, Choi JM, et al. Association of complete radiologic and pathologic response following locoregional therapy before liver transplantation with long-term outcomes of hepatocellular carcinoma: a retrospective study. *J Vascu Interven Radiol*. 2019;30(3):323–329. doi:10.1016/j.jvir.2018.11.037
22. Yang K, Sung PS, You YK, et al. Pathologic complete response to chemoembolization improves survival outcomes after curative surgery for hepatocellular carcinoma: predictive factors of response. *HPB*. 2019;21(12):1718–1726. doi:10.1016/j.hpb.2019.04.017
23. Huang C, Zhu XD, Shen YH, et al. Radiographic and α-fetoprotein response predict pathologic complete response to immunotherapy plus a TKI in hepatocellular carcinoma: a multicenter study. *BMC Cancer*. 2023;23(1):416. doi:10.1186/s12885-023-10898-z
24. Lencioni R, Llovet J. Modified RECIST (mRECIST) assessment for hepatocellular carcinoma. *Semin Liver Dis*. 2010;30(01):052–060. doi:10.1055/s-0030-1247132
25. Llovet JM, Lencioni R. mRECIST for HCC: performance and novel refinements. *J Hepatol*. 2020;72(2):288–306. doi:10.1016/j.jhep.2019.09.026
26. Zhang W, Xu AH, Wang W, Wu YH, Sun QL, Shu C. Radiological appearance of hepatocellular carcinoma predicts the response to trans-arterial chemoembolization in patients undergoing liver transplantation. *BMC Cancer*. 2019;19(1):1041. doi:10.1186/s12885-019-6265-1
27. Chapiro J, Wood LD, Lin M, et al. Radiologic-pathologic analysis of contrast-enhanced and diffusion-weighted MR imaging in patients with HCC after TACE: diagnostic accuracy of 3D quantitative image analysis. *Radiology*. 2014;273(3):746–758. doi:10.1148/radiol.14140033
28. Borde T, Nezami N, Laage Gaupp F, et al. Optimization of the BCLC staging system for locoregional therapy for hepatocellular carcinoma by using quantitative tumor burden imaging biomarkers at MRI. *Radiology*. 2022;304(1):228–237. doi:10.1148/radiol.212426
29. Han X, Wu X, Wang S, et al. Automated segmentation of liver segment on portal venous phase MR images using a 3D convolutional neural network. *Insights Imaging*. 2022;13(1):26. doi:10.1186/s13244-022-01163-1
30. Müller L, Kloeckner R, Mähringer-Kunz A, et al. Fully automated AI-based splenic segmentation for predicting survival and estimating the risk of hepatic decompensation in TACE patients with HCC. *Eur Radiol*. 2022;32(9):6302–6313. doi:10.1007/s00330-022-08737-z
31. Wei H, Zheng T, Zhang X, et al. Deep learning-based 3D quantitative total tumor burden predicts early recurrence of BCLC a and B HCC after resection. *Eur Radiol*. 2024;35(1):127–139. doi:10.1007/s00330-024-10941-y
32. Travis WD, Dacic S, Wistuba I, et al. IASLC multidisciplinary recommendations for pathologic assessment of lung cancer resection specimens after neoadjuvant therapy. *J Thorac Oncol*. 2020;15(5):709–740. doi:10.1016/j.jtho.2020.01.005
33. Aslam A, Chernyak V, Miller FH, et al. CT/MRI LI-RADS 2024 update: treatment response assessment. *Radiology*. 2024;313(2):e232408. doi:10.1148/radiol.232408